The International Journal of
Robotics Research
30(13) 1585–1595

DOI: 10.1177/0278364911408631
ijr.sagepub.com

Running with improved disturbance rejection by using non-linear leg springs

JG Daniël Karssen and Martijn Wisse

Abstract

Most running robots and running models use linear leg springs. Non-linear leg springs have the potential to improve the performance of running robots and models, but it is not clear to what extent. In this paper, the effect of non-linear leg springs on disturbance rejection behavior is investigated. The optimal leg stiffness profile is determined by optimizing the gait sensitivity norm, a measure for disturbance rejection. The results of this optimization show that the optimal leg stiffness profile is strongly non-linear, and that the disturbance rejection is a factor of seven better than it would be with the optimal linear leg stiffness. The cause for this great improvement is that non-linear leg springs allow stable limit cycles that are much further away from the fall modes.

Keywords

Running, non-linear leg stiffness, disturbance rejection

1. Introduction

For bipedal running motions, leg springs are useful, because running is a gait that is characterized by large changes in potential and kinetic energy. During the stance phase, a part of the energy can be stored in spring-like elements in the leg. These spring-like elements can help in reducing the cost of transport (Cavagna et al. 1977; Alexander 1988) and can reduce the damaging impact forces during touchdown (Liu and Nigg 2000). Human running can effectively be modeled with a simple spring–mass model, which has a spring as leg and a point mass as the body (Blickhan 1989; McMahon and Cheng 1990). The same model has also been used to design running robots with spring-like leg behavior. For some robots, this behavior is the result of having actual mechanical leg springs (Raibert 1986; Zeglin and Brown 1998; Ahmadi and Buehler 2006; Hurst and Rizzi 2008; Owaki et al. 2009). Others use actuators and control schemes to mimic spring-like leg behavior (Chevallereau et al. 2005). However, almost all of the research (both for human running and for robot running) is done with linear springs, presumably for ease of modeling, without considering the limitations of this simplifying assumption. Only two studies have looked at the effect of non-linear leg springs. Rummel and Seyfarth (2008) investigated the effect of the non-linearity introduced by the use of a two-segment leg with a linear torsion spring in the knee joint. They found that this non-linearity increases the speed range over which stable running is possible. Owaki and Ishiguro (2007) compared a linear and a quadratic leg spring and found that a quadratic leg spring results in a faster convergence to a limit cycle. Although both of these studies involved only a single (and somewhat randomly chosen) type of non-linearity, the observed performance increases were of such significance that they warrant a thorough study of all possible non-linear springs.

The key performance criterion for such a study is the disturbance rejection behavior, currently one of the main challenges for running robots due to floor irregularities, actuator limitations, and sensor noise. One might think that energetic efficiency is also important, but in the simple point mass model all linear and non-linear springs will lead to perfectly lossless motions. Therefore, we do not address efficiency, but thoroughly study the disturbance rejection behavior. The earlier studies investigated stability (Rummel and Seyfarth 2008) and convergence speed (Owaki and Ishiguro 2007), two measures that provide a partial measure for the disturbance rejection behavior. Currently, for running motions there is no complete measure, which can

Delft University of Technology, Delft, Netherlands

Corresponding author:

JG Daniël Karssen, BioMechanical Engineering, Faculty of Mechanical Engineering, Delft University of Technology, Mekelweg 2, Delft 2628 CD, the Netherlands

Email: j.g.d.karssen@tudelft.nl

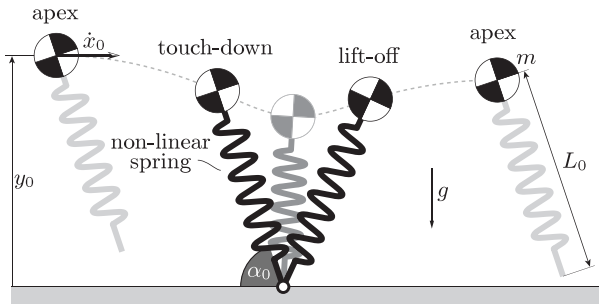

Fig. 1. A simple running model consisting of a point mass on a massless spring. In this study, the spring can have any non-linear stiffness profile. In addition to spring properties, the model has four parameters, leg length L_0, mass m, gravity constant g, and angle-of-attack α_0 and two initial conditions, apex height y_0 and apex velocity $\dot{x}_0$.

quantify the disturbance rejection behavior within a reasonable computation time. Fortunately, for walking motions such a measure (the gait sensitivity norm (Hobbelen and Wisse 2007)) has recently been introduced, which can be adapted and validated for running motions.

The goal of this paper is to find how much the disturbance rejection can really be improved if the optimal non-linear leg stiffness profile is used. We aim to provide the reader with (1) an indication of the upper bound on the disturbance rejection improvement by the use of non-linear leg stiffness, and (2) a guide towards designing optimal leg stiffness profiles. The remainder of this paper is organized as follows. Section 2 describes the simple running model with non-linear leg springs that is used in this study. Section 3 describes how the disturbance rejection behavior of this model is quantified. Next, Section 4 describes how the disturbance rejection behavior is optimized and shows the optimal stiffness profiles. The disturbance rejection behaviors of the optimal linear and non-linear leg spring profiles are compared in Section 5. The differences in disturbance rejection behavior are discussed in Section 6 and the paper ends with the conclusions in Section 7.

2. Non-linear spring–mass model

For this study, we use the simple spring–mass model, which is widely used for analyzing running motions (Blickhan 1989; Schwind and Koditschek 1997; Seyfarth et al. 2002; Ghigliazza et al. 2005; Poulakakis and Grizzle 2009). The model consists of a point mass on a massless spring (see Figure 1). Some refer to it as the spring loaded inverted pendulum (SLIP) model, because the spring describes an inverted pendulum motion during the stance phase (Schwind and Koditschek 1997). The low complexity of this model makes it suitable to study fundamental properties of running and it is shown that in spite of its low complexity it is a good model for human and robot running (Blickhan and Full 1993; Full and Koditschek 1999).

The model has two distinct phases, a flight phase and a stance phase. During the flight phase, the point mass follows a ballistic trajectory, as the spring does not apply any force. The flight phase ends and the stance phase starts when the leg touches down with a touch-down angle, called the angle-of-attack α_0. During the stance phase, the motion is given by

$$m\begin{bmatrix}\ddot{x}\\ \ddot{y}\end{bmatrix} = \begin{bmatrix}-\cos\alpha\\ \sin\alpha\end{bmatrix} F_s + \begin{bmatrix}0\\ -mg\end{bmatrix}, \tag{1}$$

where α is the angle that the leg makes with the ground and F_s is the spring force. The stance phase ends, at lift-off, when the spring leg is at its rest length L_0.

For this study, we use a constant angle-of-attack controller, which results in the same angle-of-attack for every step. The used angle-of-attack in this controller is a free parameter in the optimization.

The spring force F_s can be a linear or non-linear function of the leg compression ΔL,

$$F_s = f(\Delta L), \quad \text{with } \Delta L = L_0 - L. \tag{2}$$

The parameterization of the stiffness profile f is described in Section 4.1. In addition to the parameters for the stiffness profile, the model has four parameters: leg length L_0, mass m, gravity constant g, and angle-of-attack α_0. By means of normalization ($L_0 = 1$ m, $m = 1$ kg, $g = 1$ m s^{-2}), the number of free parameters is reduced by three, leaving only the spring profile and the angle-of-attack as free parameters.

We define the start of a step as the apex point during the flight phase. At the apex point the vertical velocity is zero and the state of the model is described by two initial conditions, apex height y_0 and horizontal velocity $\dot{x}_0$. We map the initial conditions of a step onto the initial conditions of the next step with the stride function S:

$$\mathbf{v}_{n+1} = S(\mathbf{v}_n) \quad \text{with } \mathbf{v} = \begin{bmatrix}y_0\\ \dot{x}_0\end{bmatrix}. \tag{3}$$

The stride function can have zero, one, or more fixed points, i.e. motions where the initial conditions result in the same initial conditions after one step.

$$\mathbf{v}^* = S(\mathbf{v}^*). \tag{4}$$

If the model is started in a fixed point, it will keep on repeating the same motion. This motion is called a limit cycle and in the next section, we discuss how disturbance response of a limit cycle can be quantified.

The model has two fall modes, namely a fall backwards and a trip. For a certain range of initial conditions, the behavior (i.e. falling backwards, tripping, or not falling) is determined by the stiffness profile of the leg spring, the key effect to be studied in this paper. However, beyond certain limits, a fall is sure to occur, no matter the stiffness profile. A trip surely occurs when the foot is below the ground at the apex point, which is given by

$$y_0 < L_0 \sin\alpha_0. \tag{5}$$

A fall backwards is sure to occur when the initial conditions result in a velocity vector at touchdown that points behind the foot. This limit on the initial conditions is given by

$$\begin{aligned} \tan\alpha_0 &< \frac{\dot{y}_{td}}{\dot{x}_{td}}, \\ \text{with } \dot{y}_{td} &= \sqrt{2g(y_0 - L_0\sin\alpha_0)}, \\ \dot{x}_{td} &= \dot{x}_0. \end{aligned} \tag{6}$$

These two limits are discussed and illustrated further in Section 6.1.

3. Disturbance rejection measures

In this study, we aim to optimize the disturbance rejection of the running model by adjusting the leg stiffness profile. This optimization requires a measure that quantifies the disturbance rejection. A variety of such measures is available, which we describe in Sections 3.1–3.4. Unfortunately, all of these measures are either too unrealistic or too computationally intensive for the optimization procedure. Therefore, in Section 3.5 we extensively describe the gait sensitivity norm, a measure that is both fast computable and that is a good approximation of the real disturbance behavior, but which has not previously been used for running models. Finally in Section 3.6 we summarize how the various measures are used in the remainder of the paper.

3.1. Largest allowable disturbance

The largest deterministic disturbance that a model can handle without falling is often used as a disturbance rejection measure (McGeer 1990; Pratt et al. 2001; Wisse et al. 2005). This measure quantifies the maximal disturbance a model can handle, but does not take into account the convergence rate after a disturbance. In this paper, we determine the largest allowable disturbance, for a floor height and push disturbance. These disturbances are implemented as a change in the initial conditions, which for the floor height disturbance e_{floor} is,

$$y_0 = y_0^* + e_{\text{floor}}, \tag{7}$$

$$\dot{x}_0 = \dot{x}_0^*, \tag{8}$$

and for the push disturbance e_{push},

$$y_0 = y_0^*, \tag{9}$$

$$\dot{x}_0 = \dot{x}_0^* + e_{\text{push}}, \tag{10}$$

in which y_0^* and $\dot{x}_0^*$ are the initial conditions for the limit cycle. Determining the largest allowable disturbance is computationally intensive, because it involves simulating many steps.

3.2. Largest allowable random disturbances

A better, but more computationally intensive, method to determine the disturbance rejection behavior is to disturb the model with multiple disturbances in succession instead of a single disturbance. With multiple disturbances in succession, the maximal disturbance capability and the convergence rate are both taken into account. There are many ways to define a multi-disturbances measure. In this paper, we use maximal floor height variation as defined by Hobbelen and Wisse (2007). They quantified the disturbance rejection as the maximal variance of a Gaussian white noise sequence that, when applied as successive floor height disturbances, causes the model to fall exactly four times in an 80-step trial. In this 80-step trial, the model is restarted in its fixed point after a fall. This disturbance rejection measure is noisy, due to the random disturbances it uses to test the disturbance rejection. To decrease the noise, the maximal floor height variation is calculated 10 times and averaged. The maximal floor height variation is even more computationally intensive than the largest allowable disturbance, as it involves the simulation of many 80-step trials. For our running model, it takes of the order of 10 minutes to calculate the maximal floor height variation for a single parameter set.

3.3. Basin of attraction

The total set of initial conditions that result in a steady running motion is called the basin of attraction. The shape and size of the basin of attraction indicates how sensitive the model is for initial condition changes (Schwab and Wisse 2001; Van der Linde 2001). The basin of attraction can have a highly irregular shape, making it computationally intensive to determine the exact shape, as for each possible initial condition a trail of many steps has to be run.

3.4. Floquet multipliers

The stability of the linearized step-to-step behavior is also used as indicator of the disturbance rejection behavior (Hürmüzlü and Moskowitz 1986; McGeer 1990; Strogatz 2000). This stability is expressed in terms of Floquet multipliers, which are the eigenvalues of the linearized step-to-step map A. This map A is found by linearizing the stride function S (Equation (3)) around the fixed point $\mathbf{v}^*$,

$$\Delta\mathbf{v}_{n+1} = A\Delta\mathbf{v}_n \quad \text{with } \Delta\mathbf{v}_n = \mathbf{v}_n - \mathbf{v}^*. \tag{11}$$

The Floquet multipliers indicate how fast small deviations from the limit cycle converge back to the limit cycle. A system is stable if the magnitude of all the Floquet multipliers is smaller than one. Our running model has two Floquet multipliers as it has two initial condition variables. One of these Floquet multipliers is one, due to the conservative nature of the model. An advantage of Floquet multipliers is that they require little computation time as it uses as a linearized step-to-step function. A disadvantage is that Floquet multipliers are not a good predictor of how well the model can handle large disturbances (Schwab and Wisse 2001; Hobbelen and Wisse 2007).

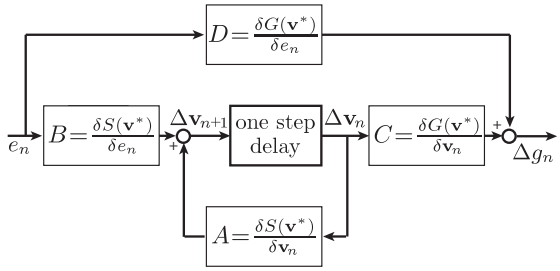

Fig. 2. Block diagram of the step-to-step discrete system that describes the relation between an input disturbance e and an output gait indicator Δg. The internal states of this system are the initial conditions to a step $\Delta\mathbf{v}$. The sensitivity matrices **A**, **B**, **C**, and **D** are the derivatives of the stride function S and the gait indicator function G to the initial condition $\mathbf{v}_n$ and the input disturbance e, respectively. Adapted from Hobbelen and Wisse (2007).

3.5. Gait Sensitivity Norm

Recently, Hobbelen and Wisse (2007) introduced the gait sensitivity norm, a new disturbance rejection measure. They showed that this measure is a good measure for the disturbance rejection performance of walking models as well as walking prototypes in the presence of real-world disturbances. The gait sensitivity norm is also fast computable, as it uses a linearized step-to-step function, which makes it useful for optimization. In this section, we will first give a short introduction of the gait sensitivity norm and then discuss the implementation and validation of this measure for our running model.

The gait sensitivity norm uses a gait indicator to predict the disturbance rejection performance. The gait indicator should quantify how likely the model is to fall. Examples of gait indicators are step time, step length and kinetic energy. The gait sensitivity norm $\|\partial g/\partial e\|_2$ is defined as the H_2-norm of the gait indicator g in the steps after a disturbance e:

$$\left\|\frac{\partial g}{\partial e}\right\|_2 = \frac{1}{e}\sqrt{\sum_{n=0}^{\infty}(g_n - g^*)^2} \tag{12}$$

in which g^* is the gait indicator in an unperturbed step and g_n is the gait indicator in the nth step after the disturbance. For model simulation studies, it is not necessary to simulate many steps, as the gait sensitivity norm can be calculated from the linearized response of the stride function:

$$\left\|\frac{\partial g}{\partial e}\right\|_2 = \sqrt{\mathrm{trace}(\mathbf{D}^{\mathrm{T}}\mathbf{D}) + \sum_{n=0}^{\infty}\mathrm{trace}(\mathbf{B}^{\mathrm{T}}(\mathbf{A}^{\mathrm{T}})^k\mathbf{C}^{\mathrm{T}}\mathbf{C}\mathbf{A}^k\mathbf{B})} \tag{13}$$

in which **A**, **B**, **C**, and **D** are the sensitivity matrices, which describe the sensitivity of the initial condition $\mathbf{v}_{n+1}$ and the gait indicator g_n to changes in the previous initial condition $\mathbf{v}_n$ and to the disturbance e_n respectively (Figure 2).

The choice of disturbance e and gait indicator g is vital to obtain a good estimation of the disturbance rejection behavior. It has been shown that floor height variations as disturbance and step time as gait indicator work well for 2D walking models (Hobbelen and Wisse 2007). For our running model, we also use step time as a gait indicator, but we do not use floor height variations as a disturbance, because the running model is an idealized, energy-conserving model. A floor height variation will result in a lasting change of the systems energy, as the system has no way of dissipating energy. The lasting energy change results in a lasting change of the step time and this results in an infinite gait sensitivity norm. To prevent this, we implement the disturbance as a height variation e_{dis} where the horizontal velocity $\dot{x}_0$ is adjusted to keep the systems energy E constant:

$$y_0 = y_0^* + e_{\mathrm{dis}}, \tag{14}$$

$$\dot{x}_0 = \sqrt{2(E - y_0^* - e_{\mathrm{dis}})}. \tag{15}$$

We have to validate the gait sensitivity norm for our running model, because it is only validated for walking models and prototypes. To validate it, we compare the gait sensitivity norm with the maximal floor height variation, over a stiffness range. We do this for both the model with a linear and the model with a non-linear leg spring. The angle-of-attack is varied with the leg stiffness, so that the comparison can be made over a large range of leg stiffness. For this, we use the relation between the angle-of-attack and the leg stiffness as found by Seyfarth et al. (2002) and depicted in Figure 13. Figures 3 and 4 show the comparison between the gait sensitivity norm and floor height variation measure. Note that the reciprocal of the gait sensitivity norm is plotted so that for both measures, it applies that the higher the value, the better the disturbance rejection. For the comparison, the absolute values are not important, as long as the two measures have a similar trend. The similarity of the trends is quantified with the correlation coefficient r^2. There is a high correlation between the gait sensitivity norm and maximal floor height variation, with $r^2 = 0.94$ for the linear spring and $r^2 = 0.88$ for the non-linear spring. This shows that the gait sensitivity norm is a good predictor of the disturbance rejection behavior for our model.

3.6. Selected measures

The maximal floor height variation is the most realistic of all of the previously discussed disturbances rejection measures, as it takes into account the maximal disturbance and the convergence rate of the full non-linear system. Unfortunately, the maximal floor height variation is unsuitable as an optimization criterion as it is computationally too intensive for an optimization with many free parameters. However, the maximal floor height variation can be approximated by the fast computable gait sensitivity norm. In this study, we first optimize using the gait sensitivity norm as optimization criterion, followed by a second optimization with a reduced number of free parameters with the maximal floor

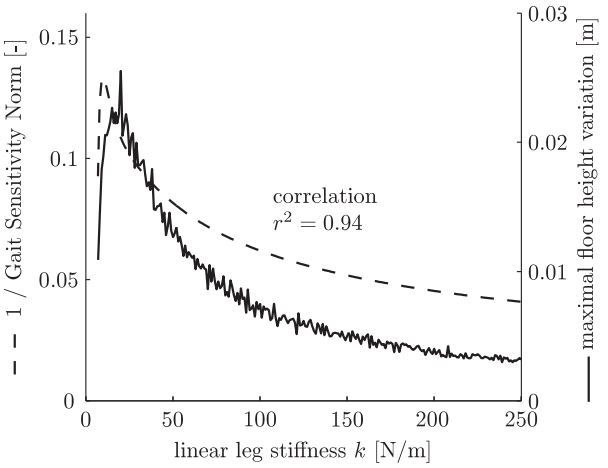

Fig. 3. Comparison between the gait sensitivity norm and the maximal floor height variation for increasing linear leg stiffness k. The model has no stable fixed points below a stiffness of 6.5 N m^{-1}. The used angle-of-attack α_0 is a function of the stiffness k, $\alpha_0 = \arcsin\left(1 - \frac{1.8}{k}\right)$. The gait sensitivity norm is highly correlated with a realistic disturbance measure, the maximal floor height variation ($r^2 = 0.94$), making it a good optimization criterion.

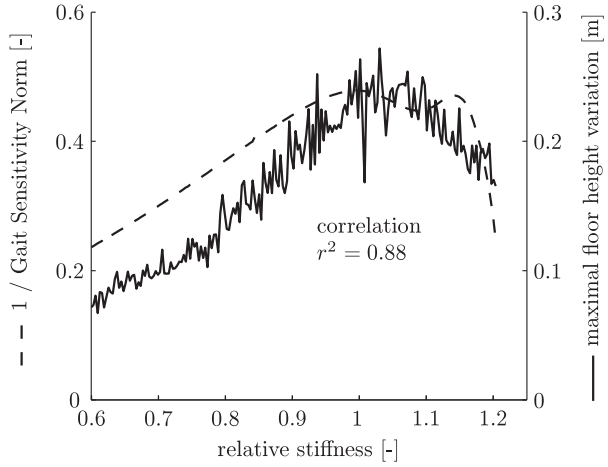

Fig. 4. Comparison between the gait sensitivity norm and the maximal floor height variation for increasing of the relative stiffness k_r of the optimal non-linear stiffness profile (Figure 7(b)). The used angle-of-attack α_0 is a function of the relative stiffness k_r, $\alpha_0 = \arcsin\left(1 - \frac{0.0011}{k_r}\right)$. The gait sensitivity norm is, also for the non-linear spring, highly correlated with the maximal floor height variation.

height variation as optimization criterion. The details of this optimization procedure are described in the next section.

4. Optimization

We optimize the disturbance rejection by adjusting the stiffness profile of the leg spring. In this section, we describe the optimization procedure (Section 4.1) and the results of two optimization studies. In the first study (Section 4.2), the disturbance rejection is optimized for a model with a non-linear stiffness profile and in the second study (Section 4.3) for a model with a linear stiffness profile.

4.1. Optimization procedure

The optimization procedure, used in this study, is inspired by the optimization procedure used by Mombaur et al. (2005). Figure 5 schematically shows the optimization procedure. The optimization function optimizes the criteria function by adjusting the stiffness profile and the angle-of-attack. The criteria function searches, for a given stiffness profile and angle-of-attack, the limit cycles of the model. This search is done by Newton–Raphson searches starting from multiple starting points to find all of the limit cycles. For most parameter combinations, the model has two limit cycles. Next, the criteria function determines for each of the limit cycles the gait sensitivity norm and returns the lowest gait sensitivity norm to the optimization function.

As optimization function, we use the Nelder–Mead simplex method. This direct search method does not use gradients. The method can handle discontinuities and not-a-number outputs of the criteria function. This makes the method suitable for our optimization problem, as the criteria function returns not-a-number for parameter sets that do not have limit cycles.

In the optimization, the system's energy is kept constant to prevent high-energy solutions, where gaits can have step lengths of many times the leg length. The constant energy level also makes the search for limit cycles easier as the number of initial condition variables is reduced to one. For this optimization study, we use an energy level of 2 J, which corresponds, when scaled to human proportions and the earth's gravitational field, to a human running at 4 m s^{-1}. In Section 6.4, we discuss the effect of the energy level on the optimization results.

The stiffness profile is parameterized with a cubic spline. The cubic spline gives a smooth profile that can be well integrated in the simulation. The cubic spline is built up using N knots. The knots are evenly distributed over the active region of the stiffness profile, in which the active region starts at zero compression to the maximal compression that occurs during the limit cycle. The knots are redistributed after a number of optimization cycles, because the active region can change during the optimization. The stiffness profile beyond the maximal compression has no influence on the motion of the model during the limit cycle or on the gait sensitivity norm and therefore this region does not need to be modeled. In Section 4.2 we discuss how the stiffness profile beyond the maximal compression is defined. As the active region can change during the optimization, the knots have to be redistributed after a number of optimization cycles. In addition to the N knot values, the slope of the start and end knot need to be specified. This results in a total of $(N + 2)$ parameters to

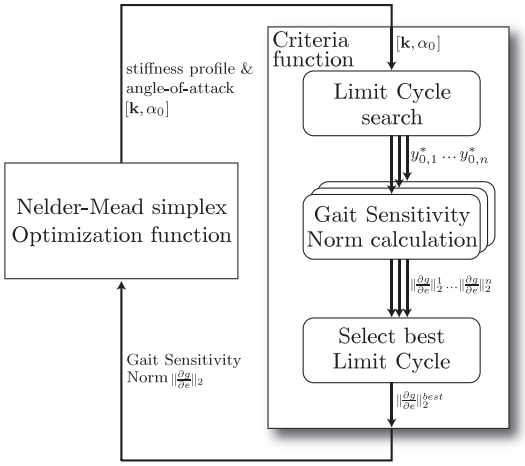

Fig. 5. Diagram of the optimization procedure. The optimization function adjusts the parameter set (spring properties and angle-of-attack) to minimize the criteria function. This criteria function determines, for a given parameter set, all fixed points and corresponding gait sensitivity norms and returns the lowest gait sensitivity norm.

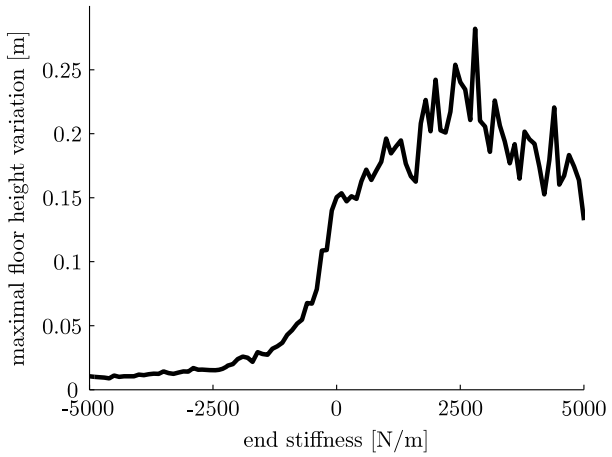

Fig. 6. The maximal floor height variation as a function of the end stiffness of the non-linear profile. The end stiffness is the slope of the stiffness profile beyond the maximal compression during a nominal step (see Figure 7(b)).

parameterize the stiffness profile. During the optimization, the number of knots is increased from 5 at the start to 10 at the end. This is done to have fast convergence in the beginning and enough freedom for the profile in the end. The optimization procedure is started at multiple starting points, in order to find the global minimum.

4.2. Optimal non-linear stiffness

The gait sensitivity norm is used as the optimization criterion to optimize the active part of the stiffness profile, from zero compression to the maximal compression during the limit cycle. Although the part of the stiffness profile beyond the maximal compression does not have any effect on the gait sensitivity norm, and therefore has not been optimized, this part of the profile does have an effect on more realistic disturbance rejection measures, such as the maximal floor height variation or the maximal step-down. To optimize the profile beyond the maximal compression, we extend the profile with a linear stiffness and optimize this stiffness using the maximal floor height variation as the criterion. We use a linear stiffness, because the computational intensity of the floor height variation measure does not allow for an optimization with more parameters. Figure 6 shows the maximal floor height variation as function of the stiffness of the non-linear profile beyond the maximal compression. The maximal floor height variation is low for negative stiffness and high for positive stiffness. The optimal stiffness is about 2,500 N m^{-1} and this is what we use for the remainder of the study.

Figure 7(b) shows the optimal non-linear stiffness profile. The profile is highly non-linear and it even has a part with a negative slope. The stiffness of the non-linear profile is high and this results in a maximal leg compression of only 2.5% of the rest length. The angle-of-attack for this non-linear profile is large; the leg is almost perpendicular to the floor at touch-down.

4.3. Optimal linear stiffness

For the linear stiffness profile, we first optimize using the gait sensitivity norm as an optimization criterion and after this optimization, we perform a second optimization step using the floor height variation measure as optimization criterion. We perform the second optimization step because in spite of the high correlation between the two measures, they do not have the optimum at the same spot (see also Figure 3). In addition, the optimization of the linear spring can use computable intensive floor height variation measure, because there are only two free parameters, stiffness and angle-of-attack.

Figure 7(a) shows the optimal linear profile and angle-of-attack and the corresponding initial conditions. The optimal linear stiffness of 21 N m^{-1} is very low compared with the optimal non-linear profile. It is two orders of magnitude lower than the overall stiffness of the optimal non-linear profile. This large difference in stiffness is related to the difference in angle-of-attack for the linear and non-linear stiffness profiles, as there is a strong correlation between angle-of-attack and stiffness (Seyfarth et al. 2002). The cause of these differences between the optimal profiles is discussed in Section 6.1.

5. Disturbance rejection of optimal linear and non-linear stiffness profiles

In Figure 8 the disturbance rejection behavior of the optimal linear spring is compared with the optimal non-linear spring using five realistic disturbance measures: maximal floor height variation, step-down, step-up, push-forward, and push-backward. The measures are implemented as discussed in Section 3. All five measures show that the

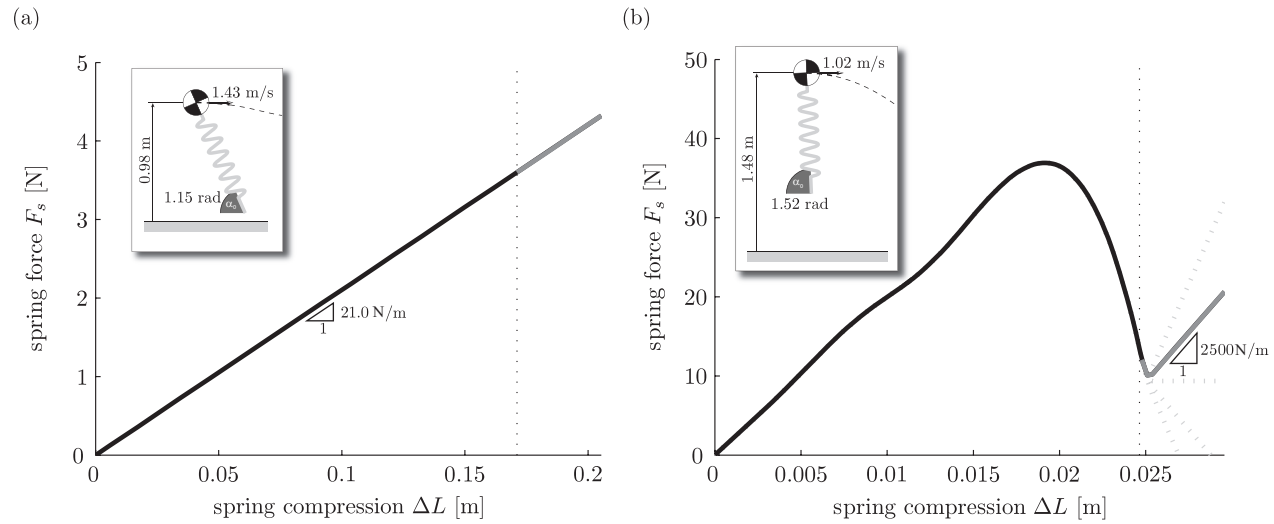

Fig. 7. The linear (a) and non-linear (b) stiffness profile for optimal disturbance rejection. The vertical dashed lines indicate the maximal compression during a nominal step. The insets show the angle-of-attack and initial conditions of limit cycles for both the profiles. Note the difference in the overall stiffness between the optimal linear (a) and non-linear (b) stiffness profile. The overall stiffness of optimal non-linear is about two orders of magnitude higher than the optimal linear stiffness.

optimal non-linear leg has a much better disturbance rejection behavior than the optimal linear leg. The model with the optimal non-linear spring can handle floor height variations with a variance of 19% of the leg length, which is a factor of seven higher than the 2.7% with the optimal linear leg spring. Figure 9 shows the trajectories of the model running on a floor with height variations. The difference in disturbance rejection is even larger for the maximal step-up. The maximal step-up is 0.485 m for the optimal non-linear spring versus 0.019 m for the optimal linear spring. This great difference is caused by the difference in apex height. At the apex point, the model with the linear spring is already close to the ground, making it sensitive for step-up disturbances. In the Section 6.1, we discuss the cause of this difference in apex height.

The difference in disturbance rejection can also be seen in the basin of attraction (Figure 10). The basin of attraction for the non-linear leg spring is much larger than for the linear leg spring, indicating that the model with the non-linear leg spring can handle larger initial condition variations. Both basins of attraction have an irregular fractal edge, which is common for simple legged systems (Schwab and Wisse 2001; Van der Linde 2001; Sato and Buehler 2005). Note that the maximal step and push disturbance are equal to the distance between the limit cycle and the edge of the basin of attraction in the vertical and horizontal direction, respectively.

6. Discussion

6.1. Explanation of the improved disturbance rejection

We showed that the model with the optimal non-linear leg spring has a much better disturbance rejection behavior compared with the optimal linear leg spring. To explain this difference in disturbance rejection behavior we have to look at what determines the disturbance rejection behavior. The disturbance rejection is determined by the combination of the following three things: (1) the disturbance sensitivity, which means how far the model deviates from its limit cycle as it is disturbed, (2) the rate at which the model converges back to its limit cycle after it is disturbed and (3) the maximal deviation from the limit cycle that the model can handle without falling.

The leg spring stiffness profile does not have any effect on the disturbance sensitivity (1), because the used floor height variation disturbance results in a change of the initial conditions that is independent of the limit cycle or the stiffness profile.

The convergence rate (2) can be expressed with the Floquet multipliers (Section 3.4). The models with a linear leg spring and a non-linear leg spring can both have a Floquet multiplier that is very close to zero, meaning that the model almost converges back to the limit cycle within a single step.

Thus, the main difference is found in the maximal deviation (3). This maximal deviation depends on the fall modes of the model. The running model has two fall modes: falling backwards and tripping (see Section 2). Figure 11 shows fall modes as a function of the initial conditions and the angle-of-attack. Note that in the indicated fall areas, the model will fall, no matter what the leg stiffness profile is. Figure 11 also shows the initial conditions and angle-of-attack for both the optimal linear and non-linear stiffness profiles. The initial condition of the non-linear profile is as far away as possible from the two fall areas, whereas the initial condition of the linear profile is close to the tripping boundary. This explains why the model with the optimal linear leg spring is far more likely to trip.

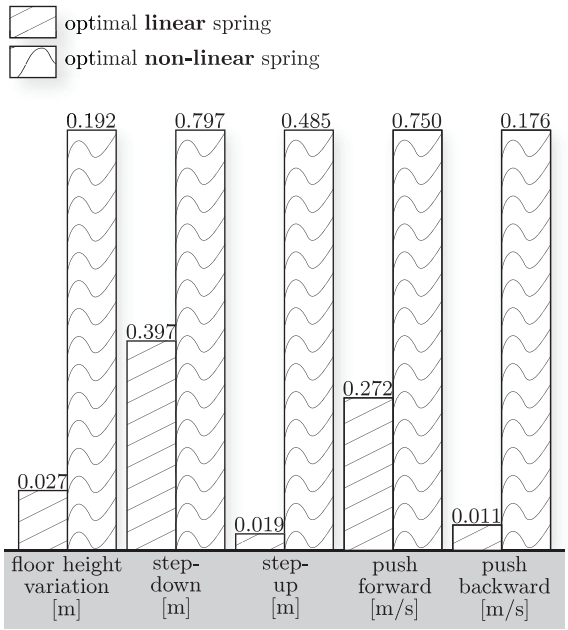

Fig. 8. Comparison of the disturbance rejection behavior between the optimal linear and non-linear leg spring. All measures show that the disturbances rejection with the non-linear spring is much better than with the linear spring.

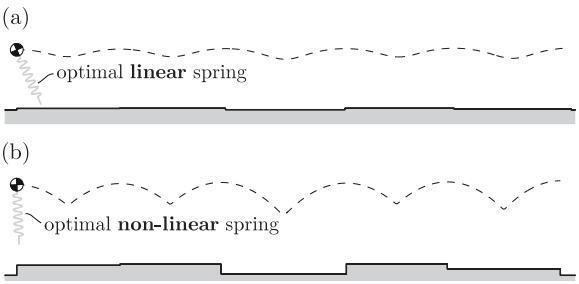

Fig. 9. The running model with the optimal linear (a) and non-linear (b) leg spring running on a floor with height variations. The dotted lines are the trajectories of the point mass. The shown floor height variations are about the maximum of what the model can handle without falling.

We hypothesize that the optimal linear spring has such a low maximal deviation because it has only one free parameter, its stiffness. With only one free parameter in the stiffness profile, the optimization can only vary two parameters, the stiffness and the angle-of-attack. However, at least three parameters are needed to obtain both an optimal convergence rate and an optimal maximal deviation. One parameter is needed for the optimal convergence rate, as the model has one controllable Floquet multiplier, and two parameters are needed for the optimal maximal deviation, one for each dimension in Figure 11. The linear spring is short one parameter, which means that there is a trade-off between the convergence rate and the maximal deviation. In this trade-off, the convergence rate should be at least such that the system is stable (the magnitude of the Floquet multiplier is lower than one). The gray area in Figure 11 indicates for which combinations of initial conditions and angle-of-attack this is the case. It shows that stable limit cycles are only possible close to the tripping boundary. This stable area also explains why the angle-of-attack for optimal linear spring is lower than for the optimal non-linear spring. For high angle-of-attacks, like the angle-of-attack of the optimal non-linear spring, the linear spring only has stable limit cycles very close to the tripping boundary.

To further test the hypothesis that the single free parameter of the linear profile is the cause for the difference in the disturbance rejection, we investigate the disturbance rejection of stiffness profiles with two free parameters. For these two-parameter profiles, one parameter is used to optimize the convergence rate, while the other parameter is used to optimize the maximal deviation. Figure 12 shows examples of these optimized two-parameter profiles. We find that it is indeed possible to have an optimal convergence rate (Floquet multiplier of zero) and an optimal maximal deviation (same initial conditions and angle-of-attack as for the optimal non-linear stiffness profile) with a two-parameter profile. Moreover, we found that the disturbance rejection, expressed in the gait sensitivity norm, of all of the optimized two-parameter profiles is almost equal to the disturbance rejection of the optimal non-linear profile (see the table in Figure 12). This means that there is not a single optimal stiffness profile, but a whole set of optimal stiffness profiles. Any non-linear stiffness profile that has the optimal convergence rate and the optimal maximal deviation will have a disturbance rejection that is very close to the optimal disturbance rejection.

The stiffness profiles in the set of optimal stiffness profiles seem to have two common characteristics, a high overall stiffness and a negative stiffness for part of the profile. The high overall stiffness is because the steep angle-of-attack requires a short contact time, which only happens with a high overall stiffness. The reason for the negative stiffness part of the optimal profiles is less clear. We believe that the negative stiffness part is because the optimal convergence rate requires that the spring force at maximal compression is low (about 10 N), while overall stiffness should be high. We do not have a mathematical proof for this requirement, despite an exhaustive search, but all of the optimal stiffness profiles we found have this characteristic.

6.2. Applicability

We showed that a non-linear stiffness profile can increase the disturbance rejection up to a factor of seven. However, we did not apply any practical constraints to the stiffness profile, as the goal of this study was to determine the upper bound on how much disturbance rejection can be improved by using non-linear leg springs. The resulting optimal non-linear stiffness profile has a gait that is almost like impulsive running (Srinivasan and Ruina 2005), with a very high leg

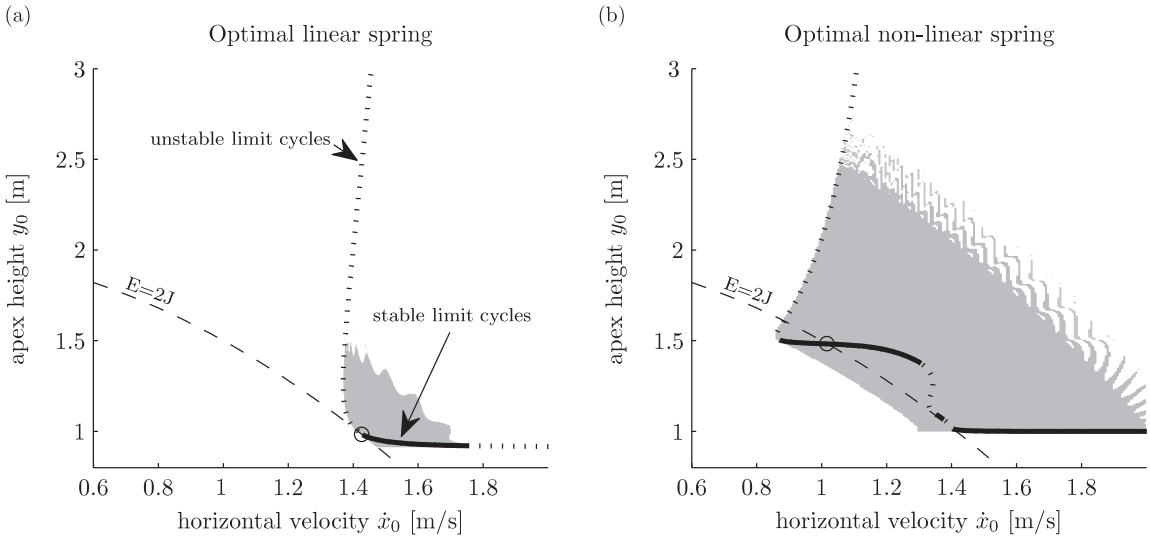

Fig. 10. The basin of attraction for the running model with the optimal linear (a) and non-linear (b) profile. The size of the basin of attraction of the optimal non-liner spring is much larger than of the linear spring, indicating that the optimal non-linear spring can handle large variations in the initial conditions.

stiffness and an angle-of-attack of almost $\pi/2$. This gait might be hard to implement on a running robot, as it results in a very short contact time. However, the method presented in this paper can also be used to determine non-linear stiffness profiles that have a good disturbance rejection and that are more practically feasible. To do this, constraints should be added to the optimization. Reasonable constraints could be a maximal stiffness or a maximal angle-of-attack. We plan to conduct such a study in the near future. In addition, we are constructing a running robot, which can be outfitted with different leg stiffness profiles. We will use this robot to validate the results of this study.

6.3. *Parameter Sensitivity*

For implementation of the optimal non-linear stiffness profile on a running robot is it important that the model is not extremely sensitive for parameter variations. Figure 13 shows how sensitive the model is for variations in the stiffness and angle-of-attack parameter for both the optimal linear and non-linear springs. The relative stiffness in this figure is a scale factor of the stiffness profile. The parameter sensitivity is approximately equal for the optimal linear and non-linear spring. With both springs, the model is sensitive for angle-of-attack variations and less so for changes in the relative stiffness. Based on these results, we can conclude that the non-linear leg spring improves the disturbances rejection while keeping the same parameter sensitivity.

6.4. *Effect of the energy level*

In the optimization there is only one parameter kept fixed, the energy level. To study the effect of this parameter on the results of the optimization, we conducted the same optimization with a higher energy level of 3 J. The optimal stiffness profile for this higher energy level has a similar shape as for the 2 J energy level. The maximal floor height variation, at this energy level, is 0.326 m for the optimal non-linear spring and 0.073 m for the optimal linear spring. This shows that also for other energy levels there are large improvements possible by using non-linear leg springs instead of linear springs.

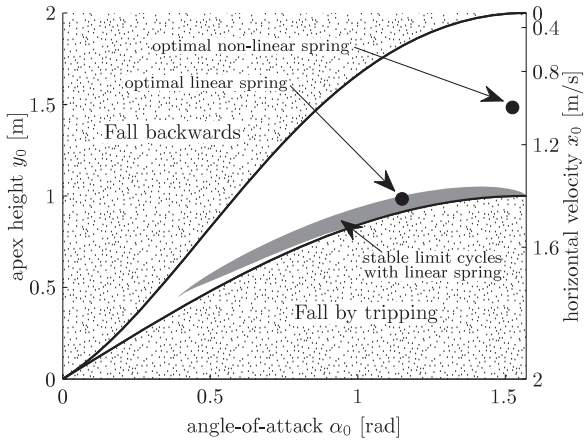

Fig. 11. The limit cycles for initial conditions y_0 and $\dot{x}_0$ and angle-of-attack α_0 combinations. In two dotted areas, limit cycles are not possible as the model will fall backwards or trip, no matter what the leg stiffness profile is. The borders of these fall areas are given in Equations (5) and (6). The gray area indicates the combinations of initial condition and angle-of-attack that have a stable limit cycle for a model with a linear leg stiffness.

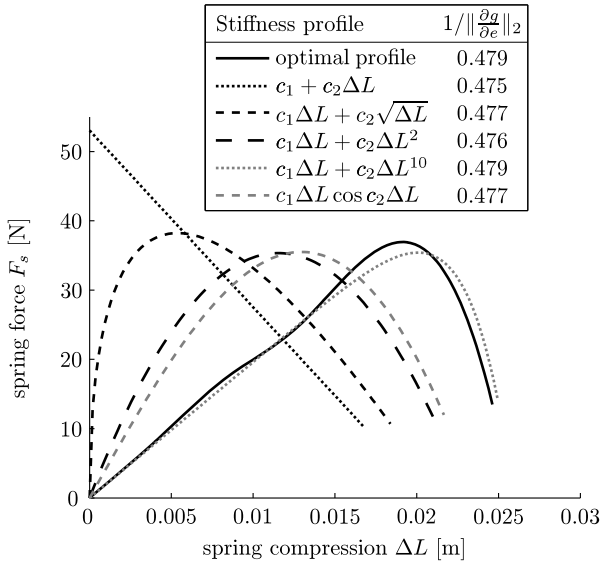

Fig. 12. The optimal non-linear stiffness profile and a set of two-parameter profiles that have almost the same disturbance rejection as the optimal non-linear stiffness profile (less than 1% difference). All profiles are shown from zero compression up to the maximal compression during the limit cycle. The table shows the disturbance rejection of the profiles as the reciprocal of the gait sensitivity norm $\|\partial g/\partial e\|_2$. Note that these profiles are examples, many more stiffness profiles exist that have a similar disturbance rejection.

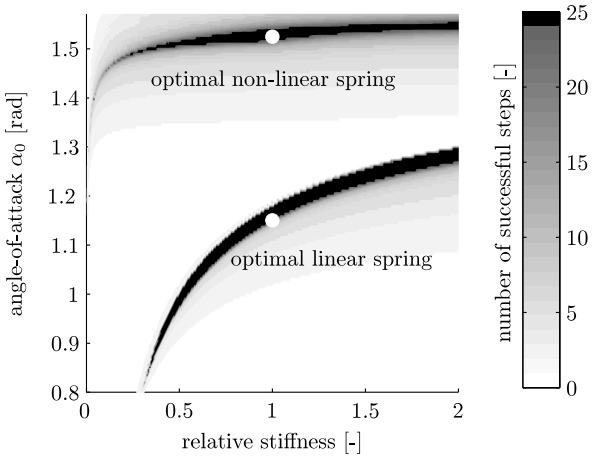

Fig. 13. The number of steps the model runs after a parameter change. The trials were stopped after 25 steps. The white dots indicate the optimal parameter combinations.

6.5. Comparisons with related studies

The results of this study are in line with the results of Rummel and Seyfarth (2008). They found that softening stiffness profiles increases the disturbance rejection. Their non-linear stiffness profiles did not have the possibility for a negative slope, which resulted in less improvement of the disturbance rejection than what we obtained in this study.

At first sight, the results might seem to be in contrast with the results of Owaki and Ishiguro (2007), as they showed improvement in stability with a stiffening profile. However, Owaki and Ishiguro (2007) looked at stability and not a disturbance rejection. This makes a large difference because it is possible to have an optimal stability (Floquet multiplier of zero) but a very poor disturbance rejection because the limit cycle is very close to the edge of the basin of attraction.

7. Conclusion

In this paper, we presented an optimization study, in which the disturbance rejection behavior of a running model was optimized by adjusting the leg spring stiffness profile. The goal of this study was to determine the optimal leg stiffness profile and to determine the upper bound on how much disturbance rejection can be improved by using non-linear leg springs. Based on the results of this study we draw the following conclusions:

- Non-linear leg springs can significantly improve the disturbance rejection of a running model. For an energy level of 2 J, the disturbance rejection can be improved up to a factor seven compared with the optimal linear leg spring (Figure 8).
- The stiffness profile for the optimal disturbance rejection behavior is strongly non-linear (Figure 7(b)).
- There is a whole set of non-linear stiffness profiles that have disturbance rejection behavior that is almost equal to the optimal disturbance rejection behavior (Figure 12).
- Non-linear leg springs allow for stable limit cycles that are further away from the fall modes compared with linear leg springs (Figure 11).
- The gait sensitivity norm is a good measure of the disturbance rejection of a running model (Figures 3 and 4).

Funding

This work was supported by the Dutch National Technology Foundation STW, applied science division of NWO.

Acknowledgements

The authors would like to thank Frans van der Helm and Matt Haberland for their help with proofreading.

References

Ahmadi M and Buehler M (2006) Controlled passive dynamic running experiments with the ARL-Monopod II. *IEEE Transactions on Robotics* 22: 974–986.

Alexander R (1988) *Elastic Mechanisms in Animal Movement*. Cambridge: Cambridge University Press.

Blickhan R (1989) The spring–mass model for running and hopping. *Journal of Biomechanics* 22: 1217–1227.

Blickhan R and Full R (1993) Similarity in multilegged locomotion: Bouncing like a monopode. *Journal of Comparative Physiology A: Neuroethology, Sensory, Neural, and Behavioral Physiology* 173: 509–517.

Cavagna G, Heglund N and Taylor C (1977) Mechanical work in terrestrial locomotion: two basic mechanisms for minimizing energy expenditure. *American Journal of Physiology—Regulatory, Integrative and Comparative Physiology* 233: 243.

Chevallereau C, Westervelt E and Grizzle J (2005) Asymptotically stable running for a five-link, four-actuator, planar bipedal robot. *The International Journal of Robotics Research* 24: 431.

Full R and Koditschek D (1999) Templates and anchors: neuromechanical hypotheses of legged locomotion on land. *Journal of Experimental Biology* 202: 3325–3332.

Ghigliazza R, Altendorfer R, Holmes P and Koditschek D (2005) A simply stabilized running model. *SIAM review* 47: 519.

Hobbelen DGE and Wisse M (2007) A disturbance rejection measure for limit cycle walkers: the Gait Sensitivity Norm. *IEEE Transactions on Robotics* 23: 1213–1224.

Hürmüzlü Y and Moskowitz G (1986) The role of impact in the stability of bipedal locomotion. *Dynamical Systems* 1: 217–234.

Hurst J and Rizzi A (2008) Series compliance for an efficient running gait. *IEEE Robotics and Automation Magazine* 15: 42–51.

Liu W and Nigg BM (2000) A mechanical model to determine the influence of masses and mass distribution on the impact force during running. *Journal of Biomechanics* 33: 219–224.

McGeer T (1990) Passive dynamic walking. *The International Journal of Robotics Research* 9: 62–82.

McMahon TA and Cheng GC (1990) The mechanics of running: How does stiffness couple with speed? *Journal of Biomechanics* 23(Suppl. 1): 65–78.

Mombaur K, Longman R, Bock H and Schloder J (2005) Open-loop stable running. *Robotica* 23: 21–33.

Owaki D and Ishiguro A (2007) Mechanical dynamics that enables stable passive dynamic bipedal running-enhancing self-stability by exploiting nonlinearity in the leg elasticity. *Journal of Robotics and Mechatronics* 19: 374.

Owaki D, Koyama M, Yamaguchi S and Ishiguro A (2009) A two-dimensional passive dynamic running biped with elastic elements. In *Dynamic Walking 2009*.

Poulakakis I and Grizzle J (2009) The spring loaded inverted pendulum as the hybrid zero dynamics of an asymmetric hopper. *IEEE Transactions on Automatic Control* 54: 1779–1793.

Pratt J, Chew C, Torres A, Dilworth P and Pratt G (2001) Virtual model control: An intuitive approach for bipedal locomotion. *The International Journal of Robotics Research* 20: 129.

Raibert M (1986) *Legged Robots that Balance*. Cambridge, MA: The MIT Press.

Rummel J and Seyfarth A (2008) Stable running with segmented legs. *The International Journal of Robotics Research* 27: 919.

Sato A and Buehler M (2005) A planar hopping robot with one actuator: design, simulation, and experimental results. In *Intelligent Robots and Systems, 2004.(IROS 2004). Proceedings. 2004 IEEE/RSJ International Conference on*, Vol. 4. Piscataway, NJ: IEEE Press, pp. 3540–3545.

Schwab A and Wisse M (2001) Basin of attraction of the simplest walking model. In *Proceedings of ASME Design Engineering Technical Conferences*.

Schwind W and Koditschek D (1997) Characterization of monoped equilibrium gaits. In *IEEE International Conference on Robotics and Automation*, pp. 1986–1992.

Seyfarth A, Geyer H, G
"unther M and Blickhan R (2002) A movement criterion for running. *Journal of Biomechanics* 35: 649.

Srinivasan M and Ruina A (2005) Computer optimization of a minimal biped model discovers walking and running. *Nature* 439: 72–75.

Strogatz S (2000) *Nonlinear Dynamics and Chaos: With Applications to Physics, Biology, Chemistry, and Engineering*. Westview Press.

Van der Linde R (2001) *Bipedal Walking with Active Springs, Gait Synthesis and Prototype Design*. PhD thesis, Delft University of Technology, Delft, The Netherlands.

Wisse M, Schwab A, van der Linde R and van der Helm F (2005) How to keep from falling forward: elementary swing leg action for passive dynamic walkers. *IEEE Transactions on Robotics* 21: 393–401.

Zeglin G and Brown B (1998) Control of a bow leg hopping robot. In *IEEE International Conference on Robotics and Automation*, pp. 793–798.